ARMY RESEARCH LABORATORY

Gleeble Testing of Tungsten Samples

by Franklyn Kellogg and Brady Butler

ARL-TR-6345 **February 2013**

NOTICES

Disclaimers

The findings in this report are not to be construed as an official Department of the Army position unless so designated by other authorized documents.

Citation of manufacturer's or trade names does not constitute an official endorsement or approval of the use thereof.

Destroy this report when it is no longer needed. Do not return it to the originator.

.

Army Research Laboratory
Aberdeen Proving Ground, MD 21005-5069

ARL-TR-6345 **February 2013**

Gleeble Testing of Tungsten Samples

Brady Butler
Weapons and Materials Research Directorate, ARL

Franklyn Kellogg
Bowhead Science and Technology

REPORT DOCUMENTATION PAGE	Form Approved OMB No. 0704-0188

1. REPORT DATE *(DD-MM-YYYY)*	2. REPORT TYPE	3. DATES COVERED (From - To)
February 2013	Final	September 2012

4. TITLE AND SUBTITLE	5a. CONTRACT NUMBER
Gleeble Testing of Tungsten Samples	5b. GRANT NUMBER
	5c. PROGRAM ELEMENT NUMBER

6. AUTHOR(S)	5d. PROJECT NUMBER
Franklyn Kellogg* and Brady Butler	5e. TASK NUMBER
	5f. WORK UNIT NUMBER

7. PERFORMING ORGANIZATION NAME(S) AND ADDRESS(ES)	8. PERFORMING ORGANIZATION REPORT NUMBER
U.S. Army Research Laboratory ATTN: RDRL-WMM-F Aberdeen Proving Ground, MD 21005-5069	ARL-TR-6345

9. SPONSORING/MONITORING AGENCY NAME(S) AND ADDRESS(ES)	10. SPONSOR/MONITOR'S ACRONYM(S)
	11. SPONSOR/MONITOR'S REPORT NUMBER(S)

12. DISTRIBUTION/AVAILABILITY STATEMENT

Approved for public release; distribution is unlimited.

13. SUPPLEMENTARY NOTES

*Bowhead Science and Technology

14. ABSTRACT

Bulk nano-grained tungsten materials produced via powder metallurgy are often too brittle for the post-processing steps required to close off porosity left after manufacturing and create a fully dense part. In order to alleviate this problem, rhenium was added to sintered nano-tungsten samples to improve ductility. A Gleeble 1500 process simulator was used to evaluate high-temperature behavior of the nano-tungsten samples, with and without rhenium, to determine a set of processing parameters that could be used during post-processing steps to create fully dense nano-grained tungsten material.

15. SUBJECT TERMS

Gleeble, tungsten, nano-grained tungsten, high-temperature testing

16. SECURITY CLASSIFICATION OF:			17. LIMITATION OF ABSTRACT	18. NUMBER OF PAGES	19a. NAME OF RESPONSIBLE PERSON
a. REPORT	b. ABSTRACT	c. THIS PAGE			Franklyn Kellogg
Unclassified	Unclassified	Unclassified	UU	36	19b. TELEPHONE NUMBER (*Include area code*) 410-306-2716

Standard Form 298 (Rev. 8/98)
Prescribed by ANSI Std. Z39.18

Contents

List of Figures

List of Tables

Acknowledgments

We would like to express our sincere thanks to Micah Gallagher (Bowhead Science and Technology) and Jim Catalano (U.S. Army Research Laboratory) for their assistance in metallographic sample preparation, and to Brad Klotz (Dynamic Science, Inc.) for his Scanning Electron Microscope expertise.

1. Introduction

The development of a bulk nano-grained tungsten material has been the subject of ongoing research at the U.S. Army Research Laboratory (ARL), Aberdeen Proving Ground, MD. While it has been shown that a powder metallurgy approach can lead to bulk nano-grained tungsten material (*1, 2*), it has been a persistent challenge to achieve full density. Commercially available tungsten must undergo complex multi-step processes (both hot and cold working) to obtain a fully dense part (*3*). Similar procedures may need to be developed to produce fully dense nano-crystalline tungsten.

One problem with post-processing procedures is that bulk nano-grained materials are often less ductile than their large grained counterparts (*4*). With conventional commercial tungsten, the brittle nature of the material is overcome by incorporating multi-step hot working procedures. However, for nano-tungsten, recrystallization and grain growth become an issue during processing at elevated temperatures. Commercially, rhenium is often added to tungsten to improve ductility and high temperature stability (*5*). By adding rhenium to nano-tungsten, enough ductility might be developed to allow for hot working at temperatures low enough to prevent grain growth.

Prior to swaging, it needs to be determined whether or not the rhenium addition does impart ductility to nano-tungsten and, if so, at what temperatures and conditions. In order to test the mechanical properties of nano-tungsten with rhenium at high temperatures, the Gleeble unit (a digital version of the 1500 model produced by Dynamic Systems Incorporated, Poestenkill, New York) at ARL was used. The Gleeble is a process simulation machine designed to mimic the thermal and mechanical conditions that arise during processing (*6, 7*). For compression testing at temperature, the Gleeble was chosen over an Instron (electromechanical test frame produced by Instron, Norwood, Massachusetts) because it can handle higher temperatures, has faster heating rates, and Gleeble experiments can be easily run in a vacuum and prevent oxidation during testing.

2. Objectives

The goals of the Gleeble experiments were: (1) establish mechanical strengths for nano-tungsten samples developed at ARL with and without rhenium and compare to conventional commercially available tungsten, (2) establish whether or not the rhenium imparts the ductility needed to post-process nano-tungsten samples, and (3) establish the post-processing conditions (temperature and force) needed to fully densify nano-tungsten.

3. Procedure

Nano-tungsten rods produced via powder metallurgy at ARL and containing 0%, 5%, and 10% rhenium were selected for Gleeble experimentation. Cylindrical samples were machined from the rods using wire electrical discharge machining (EDM); the test samples had a diameter of 7 mm and a length of 7 mm. The sample sizes were chosen to maximize the number of samples available from each rod while maintaining a length to diameter ratio of 1.0. Conventional tungsten rods (purchased from Buffalo Tungsten in Depew, New York) were sectioned into cylindrical samples with a diameter of 10 mm and a length of 15 mm. These samples were chosen to provide a general comparison to fully dense, coarse grained tungsten; it was deemed impractical to machine them down to the same dimensions as the nano-tungsten samples.

For compression testing, the Gleeble used two steel anvils with removable tungsten carbide inserts. The inserts were 19.05 mm (0.75 in) in diameter and 25.4 mm (1 in) long; they were purchased from North American Carbide in Orchard Park, New York. The anvils were anchored in place in two jaws; the left jaw is mobile and the right one is stationary. Prior to testing, the inserts were coated with graphite paint, which acted as a conductive lubricant to minimize secondary tensile stresses caused by friction. Before the paint dried, graphite foil was affixed to the center of the front face of the inserts; the foil was intended to behave as a diffusion barrier to prevent the tungsten samples from fusing to the tungsten carbide inserts at elevated temperatures. After the anvils were prepared, the sample was placed in the test chamber and held in place with a compressive load of 200 kgf.

Prior to loading the sample, an L-gauge (a linear variable differential transformer designed to interface with the Gleeble) was attached to measure strain across the sample during testing. The L-gauge was used because it is believed to provide a more accurate strain measurement than using the machine stroke, which measures displacement across the entire system. It can be used here to get an understanding of the compliance in the Gleeble system and determine if data collected using the machine stroke is as accurate. The L-gauge was calibrated before each experiment by comparing the actual and measured displacement of the anvils. Figure 1 shows a simplified cartoon schematic of the Gleeble and figure 2 is a photograph of a sample loaded into the Gleeble with the L-gauge installed.

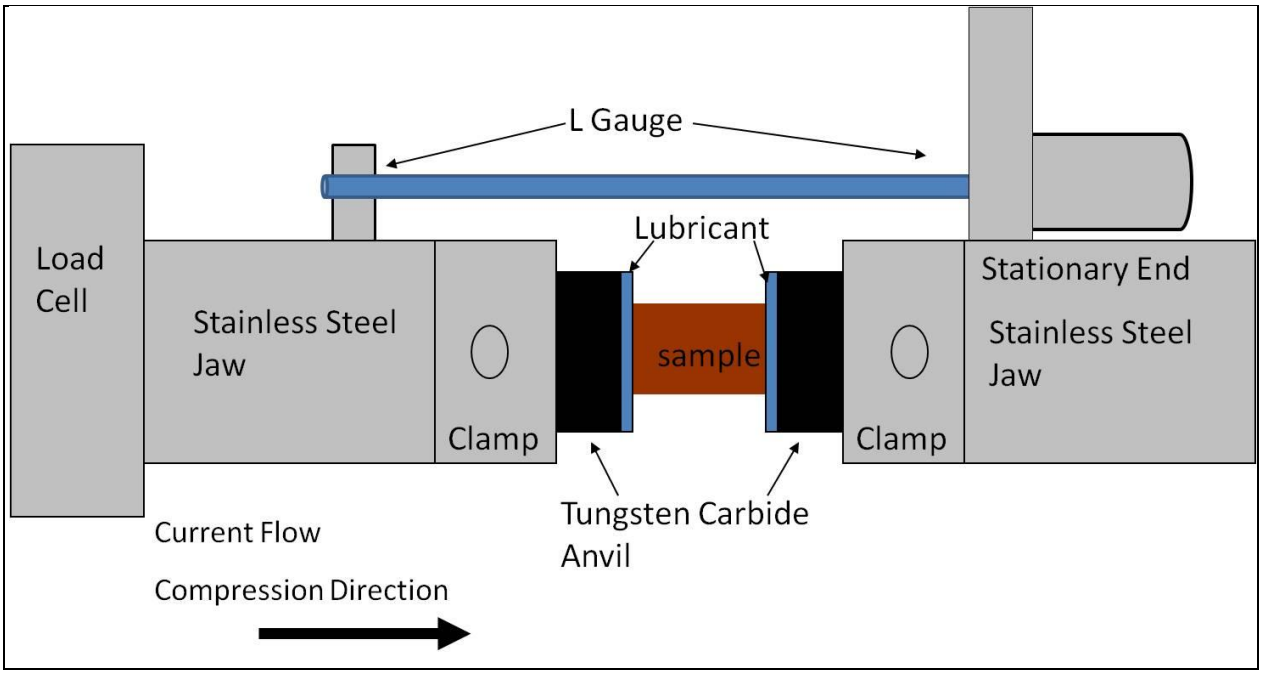

Figure 1. A schematic cartoon showing a Gleeble compression test.

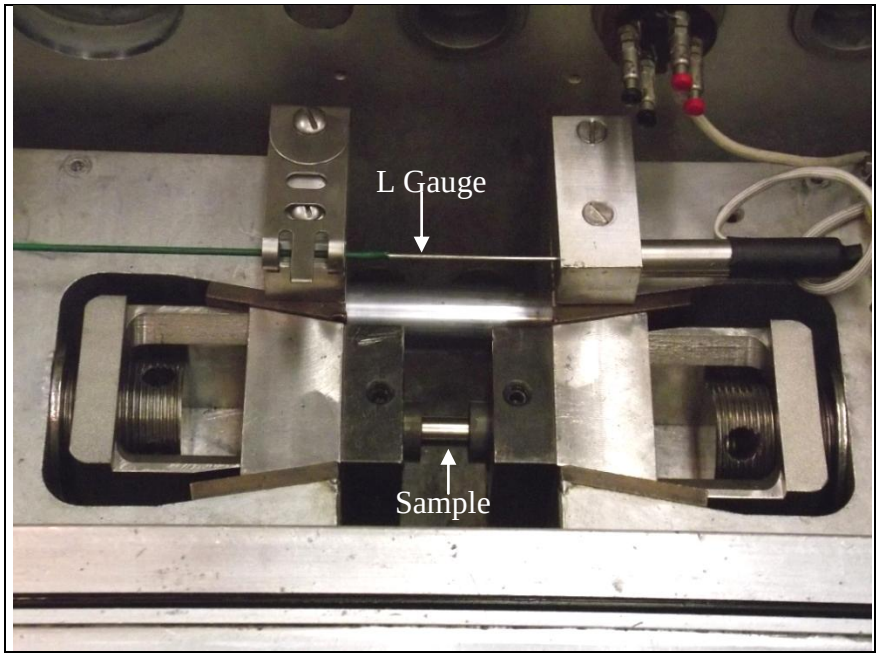

Figure 2. A tungsten sample loaded into the Gleeble.

After loading a sample, we positioned and focused the pyrometer. Prior to running the experiments, a test sample was used to calibrate the pyrometer. Thermocouples were welded to the surface of the test sample, and then a current was passed through the anvils to heat the sample via Joule heating. During calibration, the pyrometer's emissivity was adjusted until the output of the pyrometer matched the output of the thermocouples. The pyrometer is preferred

over the thermocouples because the thermocouples tend to detach from the sample during compression testing. For testing, the pyrometer was positioned to focus on the sample near the stationary jaw, ensuring that the pyrometer remained focused on the sample as it compressed (figure 3).

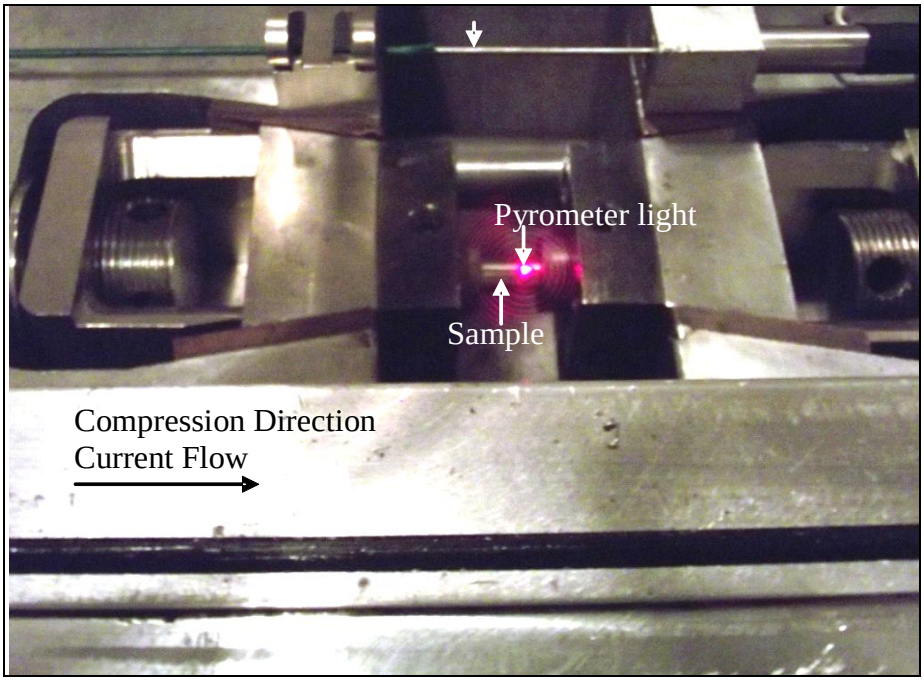

Figure 3. A sample loaded into the Gleeble. The red dot is from the pyrometer focusing laser pointer.

Once the pyrometer was set up, a glass top was put into position closing off the Gleeble's test chamber, and the vacuum system was engaged. The chamber was pumped to a vacuum level between 1 and 5 militorr then evacuated and purged with argon three times before each test.

The nano-tungsten-based samples were compressed 3 mm (43% of the total sample length) in 20 s; this corresponds to a strain rate of $2*10^{-2}$ s^{-1}. The commercial samples were compressed 6.43 mm (43% of the total sample length) in 20 s, which also corresponds to a strain rate of $2*10^{-2}$ s^{-1}. Samples were compressed at 1000, 1100, 1200, and 1300 °C. The samples were first heated to 400 °C by applying a constant current in order to heat the sample to the low end of the effective measurement range of the pyrometer (350 to 2600 °C). At 400 °C, the Gleeble was switched to pyrometer control and the applied current was automatically adjusted to achieve the programmed temperature in 3 min. During testing, force, temperature, and displacement (both across the machine [stroke] and across the jaws [L-Gauge]) were collected. True Stress and True Strain were determined during testing using the following formulas:

$$True\ Stress = \frac{Force}{\left(\frac{\left(\frac{\pi d_o^2}{4}\right)L_o}{L_o+\Delta L}\right)} \quad (1)$$

and

$$True\ Strain = ln\left(\frac{L_o+\Delta L}{L_o}\right), \quad (2)$$

where ΔL is collected as displacement (either machine stroke or L-Gauge values can be used) and d_o and L_o are the starting diameter and length of the sample. Density measurements were also taken before and after testing using Archimedes principle.

Samples were also tested at room temperature on an Instron load frame with a 222.41 kN (50 kip) load cell. The samples were compressed at the same strain rate as on the Gleeble.

Microscopy was used to identify any microstructural changes that occurred during testing either from temperature or mechanical effects. Representative samples of the consolidated tungsten before and after testing were chosen based on which samples showed the most compression. Microscopy images were taken along the compression plane (along the length of the sample in the direction of compression during testing) and in the transverse plane (perpendicular to the compression plane) as shown in figure 4.

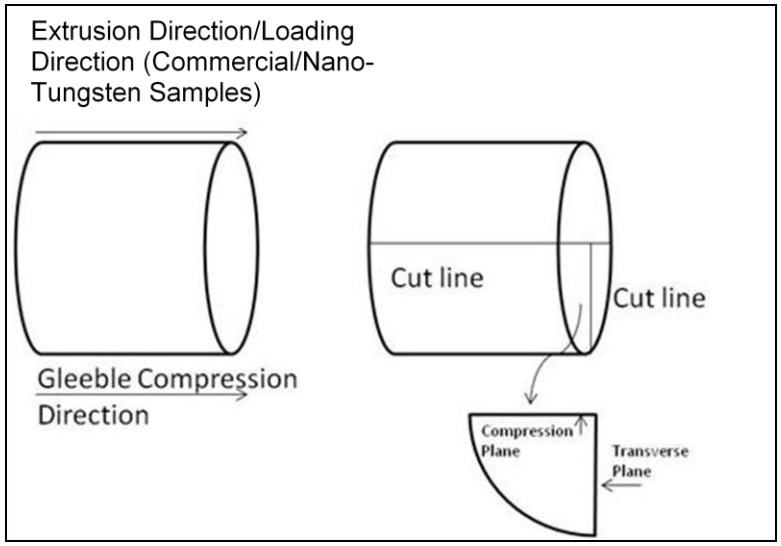

Figure 4. A cartoon schematic showing how samples were cut for microscopy.

4. Results and Discussion

Table 1 shows the densities of the samples produced at ARL.

Table 1. Density prior to and after compression testing.

Sample ID	% RE	Initial Density (cm^3)	Density after Compression (cm^3)	% Change in Density	Test Temperature
NT1	0	18.08	18.27	1.06	1000
NT3	0	18.29	18.42	0.68	1100
NT4	0	17.98	18.31	1.79	1200
NT5	0	18.24	18.50	1.41	1300
NT6[a]	0	18.69	—	—	RT
S10	5	18.66	18.43	–1.22	1000
S5	5	18.82	18.33	–2.68	1100
S4	5	18.68	18.72	0.2	1200
S3	5	18.52	18.41	–0.59	1300
S9	5	18.68	—	—	RT
T1	10	18.22	18.52	1.57	1000
T2	10	18.43	18.64	1.09	1100
T3	10	18.71	18.19	–2.87	1200
T4	10	18.47	18.38	–0.51	1300
T5	10	18.29	—	—	RT

[a]Density for sample NT6 taken from tungsten rod after sintering and prior to machining.

The initial sample density varied from 17.981 to 18.819 cm^3 depending on the sample type and processing condition which is ~93.41% to 97.76% of the theoretical density of pure tungsten (19.25 cm^3). Density variation within the same sample group was likely the result of non-uniform densification during the sintering process. Post-compression density measurements were not possible for the samples tested at room temperature because the samples were crushed into pieces too small to accurately measure density. Some of the post-compression density measurements were made on sample pieces remaining after sectioning for microscopy (samples S3, S4, S5, S10, T3, T4, and NT3). This may be the reason that samples S3, S5, T3, and T4 showed decreases in density after compression. If there was non-uniform densification during the sintering process, the sample pieces used for measuring post-compression density may have come from a portion of the sample that underwent less densification than other portions of the same sample. Overall, the changes in density after compression are small enough to be considered negligible and do not match the theoretical density.

4.1 Nano-Tungsten

The results for the compression of the nano-tungsten samples are shown in tables 2 and 3 and figure 5. During testing, sample NT1 fractured, and the room temperature (RT) sample NT6 was crushed. Sample NT6 was tested on the 222.41kN (50 kip) Instron frame.

Table 2. Compression results for nano-tungsten.

Sample	Temperature (°C)	Compression at Yield (mm)	L-Gauge Compression at Yield (mm)	Yield Stress (MPa)	Strain at Yield	L-Gauge Yield Stress (MPa)	L-Gauge Strain at Yield
NT1	1000	1.84	0.43	1060.8	0.305	1588.99	0.06
NT3	1100	1.57	0.53	878.72	0.253	1266.53	0.07
NT4	1200	1.28	0.67	522.37	0.198	724.83	0.09
NT5	1300	0.29	0.18	149.10	0.394	165.30	0.02
NT6	RT	1.08	—	4076.31	0.163	—	—

Table 3. Stroke and L-gauge displacement measurements for nano-tungsten tests.

Sample	Temperature (°C)	Change in Stroke (mm)	Change in L-Gauge (mm)	Change in Sample Length (mm)	% Change in Sample Length
NT1	1000	2.97	1.47	1.24	17.78
NT3	1100	2.98	2.08	1.63	23.29
NT4	1200	2.97	2.18	1.19	16.93
NT5	1300	2.97	2.45	0.82	11.65

At 1100 °C grain deformation was observed in the nano-tungsten sample (figure 13). While this was not observed in the nano-tungsten samples with rhenium, the onset of grain deformation at or around 1100 °C could be an explanation for the decrease in strength at temperatures over 1100 °C for the nano-tungsten material.

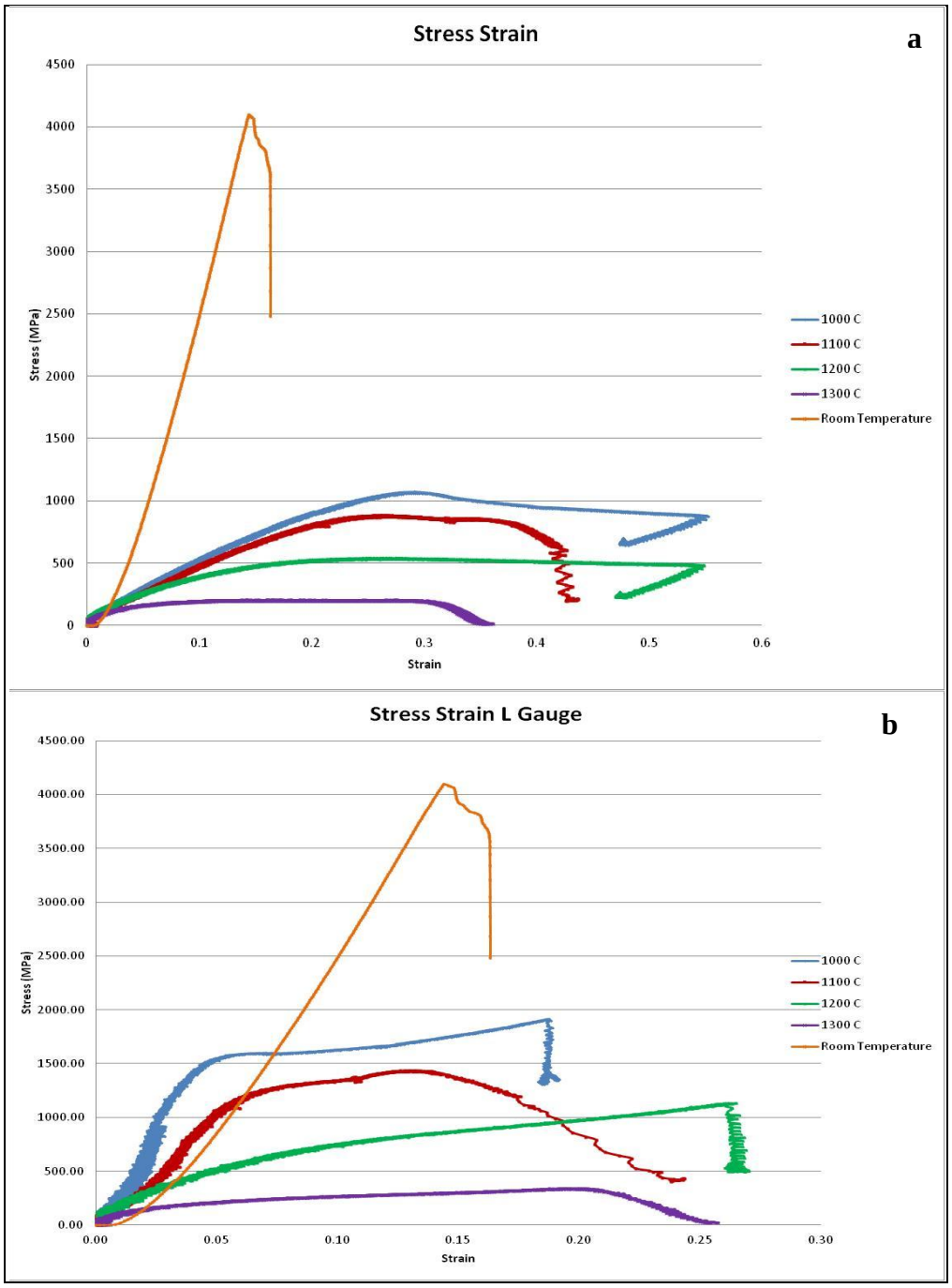

Figure 5. True stress-strain curves for nano-tungsten samples using stroke data (a) and L-gauge data (b).

4.2 Tungsten With Rhenium

The results for the compression of the nano-tungsten with 5% rhenium samples are shown in tables 4 and 5 and figure 6. Sample S9, was crushed when tested at room temperature on the Instron. Sample S14 fractured during testing.

Table 4. Compression results for nano-tungsten with 5% rhenium.

Sample	Temperature (°C)	Compression at Yield (mm)	L-Gauge Compression at Yield (mm)	Yield Stress (MPa)	Strain at Yield	L-Gauge Yield Stress (MPa)	L-Gauge Strain at Yield
S14	1000	1.99	0.43	1245.20	0.334	1918.07	0.059
S5	1100	1.73	0.46	914.54	0.291	1185.39	0.068
S4	1200	1.59	0.56	715.60	0.259	888.59	0.084
S3	1300	1.27	0.70	445.20	0.207	512.83	0.11
S9	RT	1.20	—	2833.19	0.169	—	—

Table 5. Stroke and L-gauge displacement measurements for nano-tungsten samples with 5% rhenium.

Sample	Temperature (°C)	Change in Stroke (mm)	Change in L-Gauge (mm)	Change in Sample Length (mm)	% Change in Sample Length
S14	1000	2.62	1.02	0.69	9.83
S5	1100	2.97	1.56	1.30	18.71
S4	1200	2.98	1.82	0.55	7.81
S3	1300	2.99	2.21	1.45	20.88

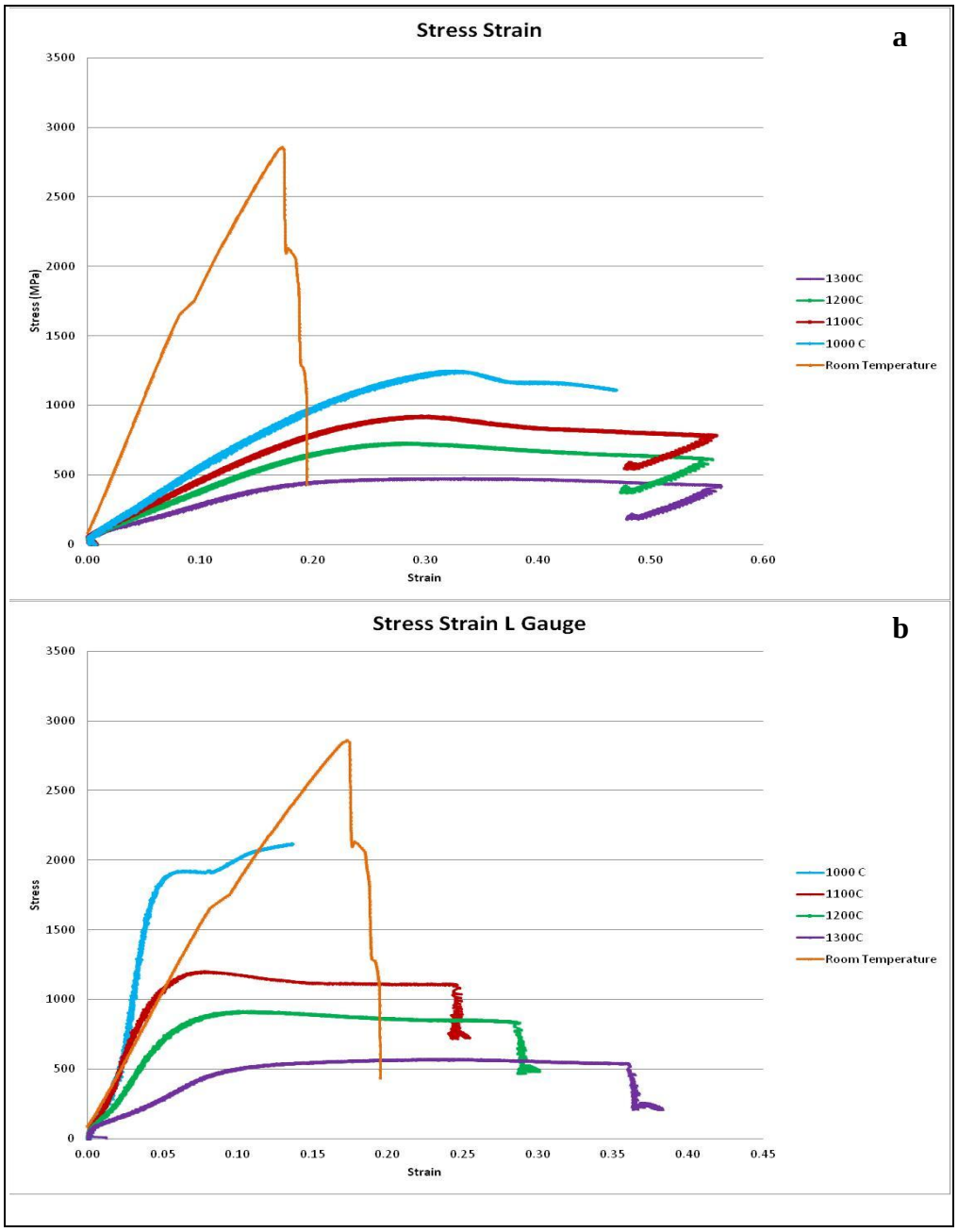

Figure 6. True stress-strain curves for nano-tungsten samples with 5% rhenium using stroke data (a) and L-gauge data (b).

The results for the compression of the nano-tungsten samples with 10% rhenium are shown in tables 6 and 7 and figure 7. The sample tested at 1300 °C, T4, partially embedded into the tungsten carbide (WC) inserts during testing. T1, the sample tested at 1000 °C, cracked during testing. Sample T5, tested at room temperature, was crushed during testing on the Instron.

Table 6. Compression results for nano-tungsten with 10% rhenium.

Sample	Temperature (°C)	Compression at Yield (mm)	L-Gauge Compression at Yield (mm)	Yield Stress (MPa)	Strain at Yield	L-Gauge Yield Stress (MPa)	L-Gauge Strain at Yield
T1	1000	1.99	0.51	1109.90	0.33	1724.14	0.070
T2	1100	1.55	0.53	897.92	0.25	1290.82	0.072
T3	1200	1.29	0.64	585.82	0.20	813.71	0.087
T4	1300	1.69	1.36	313.73	0.28	512.75	0.18
T5	RT	1.08	—	5041.59	0.28	—	—

Table 7. Stroke and L-gauge displacement measurements for nano-tungsten samples with 10% rhenium.

Sample	Temperature (°C)	Change in Stroke (mm)	Change in L-Gauge (mm)	Change in Sample Length (mm)	% Change in Sample Length
T1	1000	2.97	1.38	0.97	13.81
T2	1100	2.98	1.81	1.69	23.99
T3	1200	2.99	2.14	1.78	25.26
T4	1300	2.99	2.52	1.38	19.64

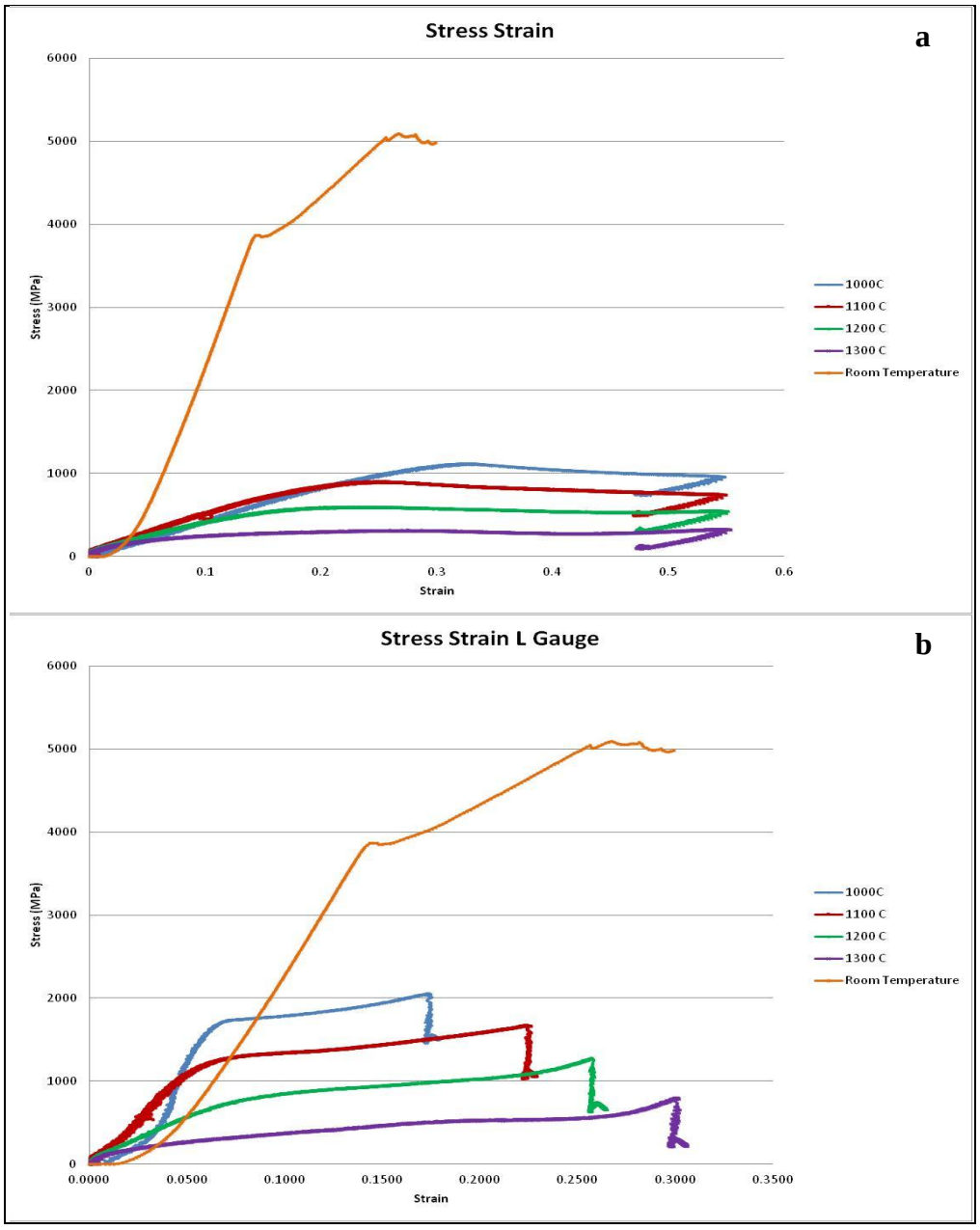

Figure 7. True stress-strain curves for nano-tungsten samples with 10% rhenium using stroke data (a) and L-gauge data (b).

At room temperature, the 10% rhenium sample had the highest yield stress, followed by the nano-tungsten and the 5% rhenium samples. At 1000 °C, the 5% rhenium sample had the highest yield stress followed by the 10% rhenium sample and the nano-tungsten sample. This trend was observed at 1100, 1200, and 1300 °C. It is clear that the addition of rhenium to the nano-tungsten sample led to increased strength and increased strength retention at high temperatures.

4.3 Commercial Tungsten

The results for the compression of commercially available samples are shown in tables 8 and 9 and in figure 8. At 1300 °C, the samples deformed the WC inserts; therefore, it was not possible to collect data at this temperature from the commercial tungsten samples. The room temperature sample (BRT) was crushed during testing.

Table 8. Compression results commercial tungsten.

Sample	Temperature (°C)	Compression at Yield (mm)	L-Gauge Compression at Yield (mm)	Yield Stress (MPa)	Strain at Yield	L-Gauge Yield Stress (MPa)	L-Gauge Strain at Yield
B5	1000	0.69	0.25	182.96	0.05	195.48	0.02
B3	1100	0.82	0.42	192.83	0.06	206.16	0.03
B7	1200	0.45	0.22	138.52	0.03	151.18	0.02
BRT	RT	1.05	—	1817.55	0.09	—	—

Table 9. Stroke and L-gauge displacement measurements for commercial tungsten samples.

Sample	Temperature (°C)	Change in Stroke (mm)	Change in L-Gauge (mm)	Change in Sample Length (mm)	% Change in Sample Length
B5	1000	6.41	5.30	5.18	34.73
B3	1100	6.41	5.46	4.96	33.26
B7	1200	6.41	5.76	5.03	33.77

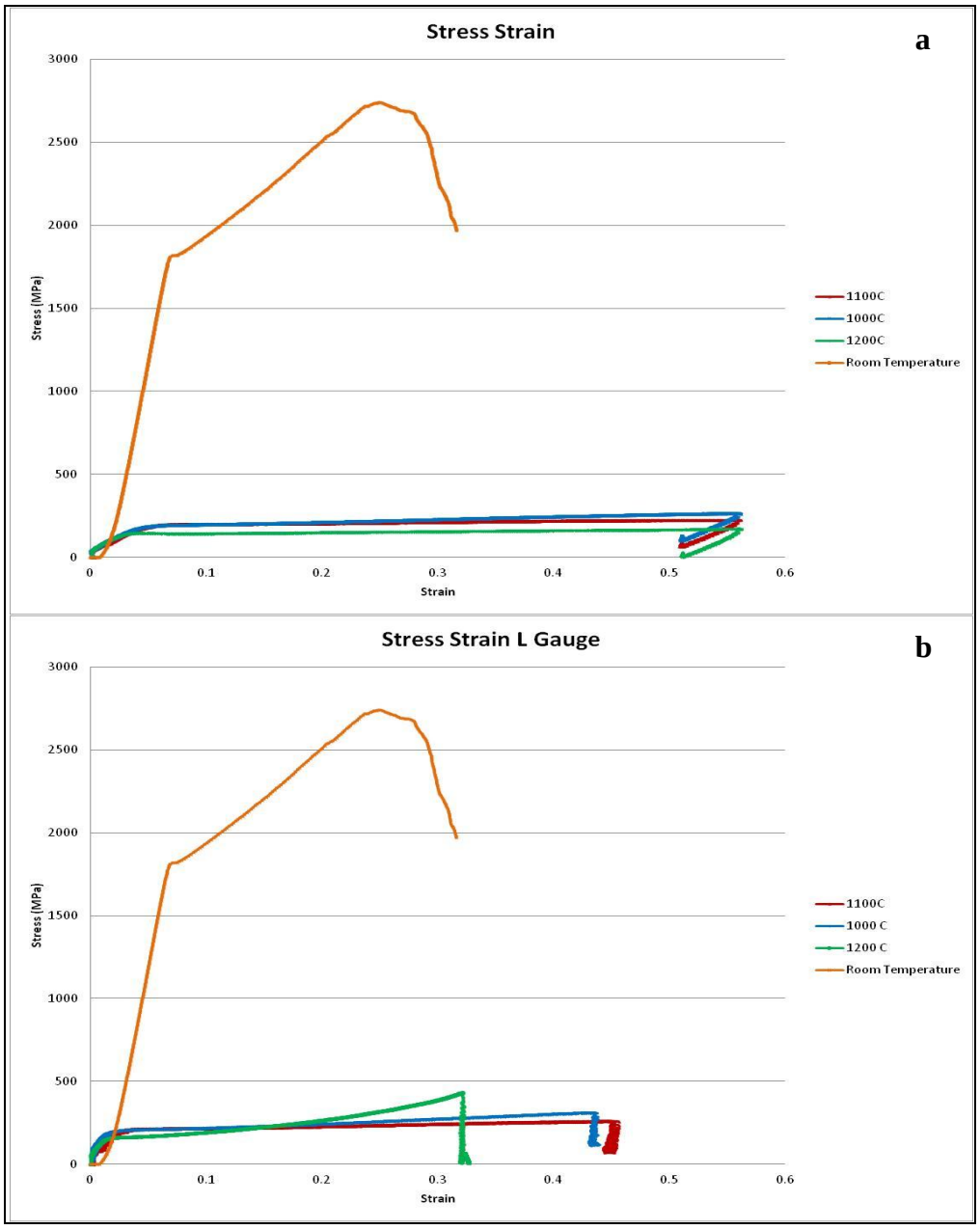

Figure 8. True stress-strain curves for commercial tungsten samples using stroke (a) and L-gauge data (b).

The commercial tungsten samples failed at the lowest loads and stresses. They also underwent the largest percent changes in sample length during deformation, showing the most ductility. The nano-grained tungsten samples, with and without rhenium, yielded at much higher loads with less strain to yield.

4.4 L-Gauge and Stroke Comparison

Throughout the results, there are significant differences between the data collected using machine stroke and L-gauge displacement. These are listed in tables 2, 4, 6, and 8 along with the changes in sample length after compression as shown in figures 5–8. Since the displacement measured by the L-gauge is much less than the displacement from machine stroke, it makes sense that the true yield stresses calculated from the L-gauge data are higher; the same force is being applied to a sample with a smaller calculated diameter. For each sample, the displacement of the L-gauge is closer to the actual deformation of the sample than the machine stroke displacement. This implies that the L-gauge does not sense many of the compliance issues inherent in the motion of the Gleeble (for example, slack from the hydraulic ram). Although the L-gauge measurements are more accurate than stroke measurements in representing the final measured compression of the sample, there are still some discrepancies between the L-gauge measurements and the measured compression of the samples (likely a result of friction or thermal expansion).

4.5 Temperature Effects

The stress-strain curves at each of the test temperatures for the different tungsten samples measured via machine stroke are shown in figure 9 and via the L-gauge in figure 10. The room temperature results from the Instron are shown in figure 11.

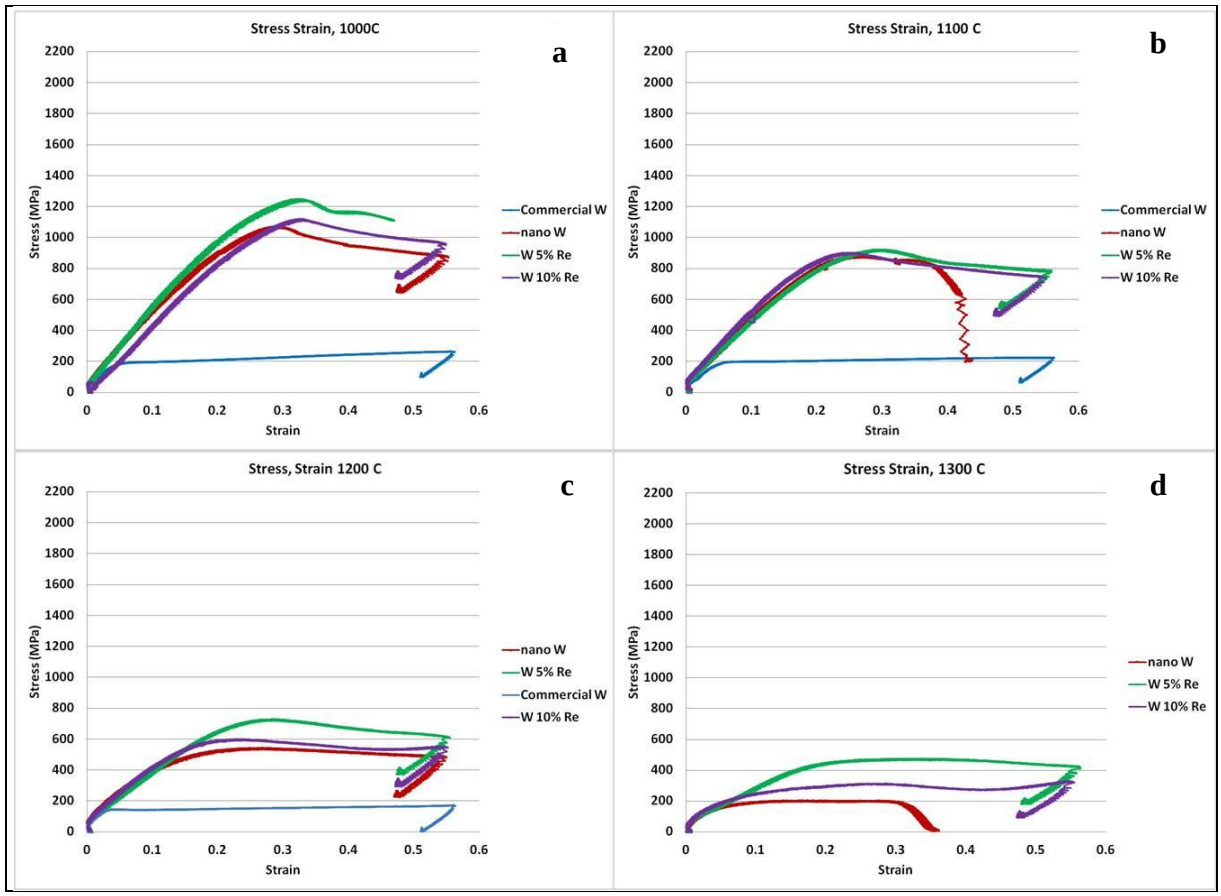

Figure 9. True stress-strain data using stroke measurements for each tungsten sample at 1000 (a), 1100 (b), 1200 (c), and 1300 °C (d).

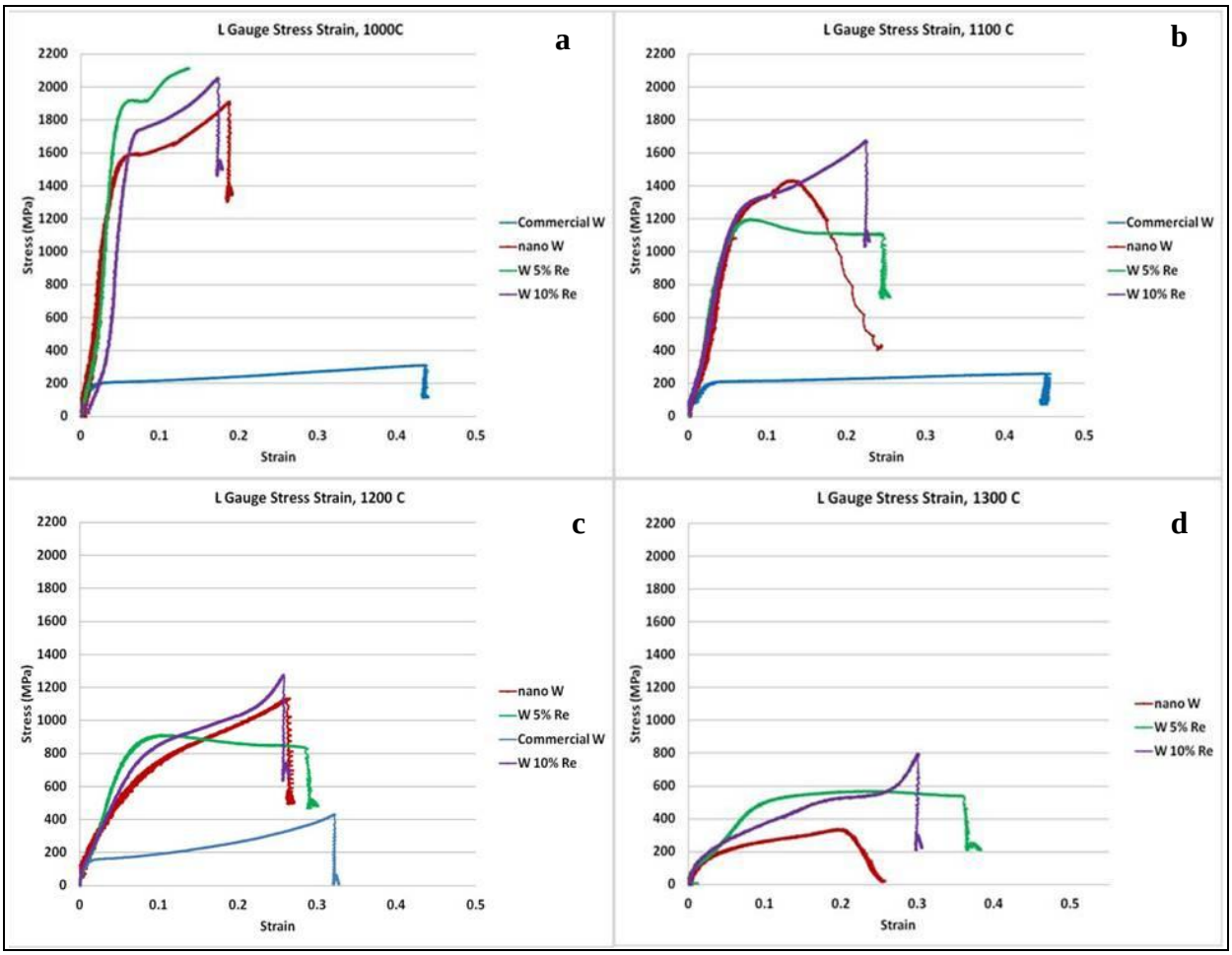

Figure 10. True stress-strain data using L-gauge measurements for each tungsten sample at 1000 (a), 1100 (b), 1200 (c), and 1300 °C (d).

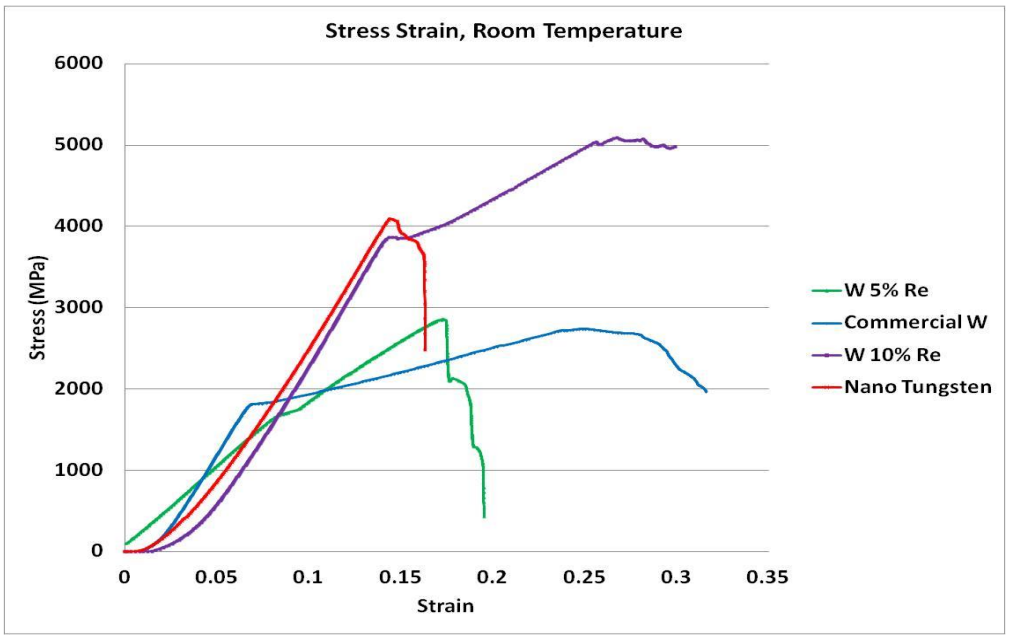

Figure 11. True stress-strain data measured at room temperature on the Instron.

The 5% rhenium samples had the highest yield stress at all temperatures tested except for the room temperature tests (at 1100 °C the 5% rhenium sample had the highest yield stress as measured by the machine stroke but not as measured by the L-gauge). The slope for the 5% sample is different from the other samples; this may have been caused by the failure of the compression platens used with the Instron during this test. It is not clear why the 5% rhenium samples had higher yield strengths than the 10% rhenium samples at elevated temperatures. As shown in table 1, there were no significant differences in the densities of the 5% and 10% rhenium samples. At room temperature, different deformation mechanisms are active than at high temperatures, which may explain why the 10% rhenium sample had the highest yield strength at room temperature. The failure of the compression platens when testing the 5% rhenium sample may have also been an influence (based on other tests, this may only be of minimal impact).

It is not clear from the data how much ductility has been imparted from the addition of rhenium. At room temperature, the 10% rhenium sample failed at a strain value very close to the failure strain of the commercial tungsten, both of which had much higher strain at failure values than the nano-tungsten or 5% rhenium samples (the 5% rhenium sample did have a higher strain at failure than the nano-tungsten sample). During Gleeble testing, the samples were not tested to failure. At 1000 °C, all of the samples except for the commercial tungsten sample cracked during testing. At 1100 to 1300 °C, the samples did not crack. The 10% rhenium samples did exhibit the second largest percentage change in sample length after compression (the commercial tungsten samples showed the most), followed by the nano-tungsten and 5% rhenium samples, respectively. However, from the scatter in the data and the low number of data points used, it

may not be prudent to draw any significant conclusions about the ductility of the samples at high temperatures. It should be noted that the nano-tungsten samples had some residual porosity as indicated by the final density of each sample. The size, concentration and morphology of these defects affect the ductility of each sample by enhancing the probabilities of crack initiation and propagation. At room temperature, it appears that the addition of rhenium improved the ductility of the nano-tungsten and approached that of commercial, large grained tungsten with 10% rhenium. In figure 11, there is a sharp bend in the 10% rhenium curve (at a strain of about 0.15) followed by an increase in the applied stress until another sharp bend occurs at an approximate strain of 0.25. This lower (first) yield point has been observed to occur without cracking while the second yield point has been observed to coincide with cracking. This behavior was observed during subsequent testing of samples of smaller size but the same composition as the 10% rhenium samples. This yield point behavior is commonly seen in body centered cubic (BCC) metals and can be attributed to dislocation mobility theories (*8*). The basic principles are that the dislocations present within the crystal structure are locked in place by solute atoms until an applied stress provides the energy for the dislocations to break free and move. This dislocation mobility is a sign that the material has some ductility and is able to flow without cracking. This behavior was also seen in the commercial tungsten sample. Neither the 5% rhenium sample nor the nano-tungsten sample exhibited this behavior of two yield points, showing an overall lack of ductility.

4.6 Microscopy

4.6.1 Nano-Tungsten Samples

The tungsten samples that showed the most compression (the largest changes in length) were sectioned for microscopy. Figure 12 shows the microstructures of nano-tungsten sample NT3 as processed and after Gleeble testing.

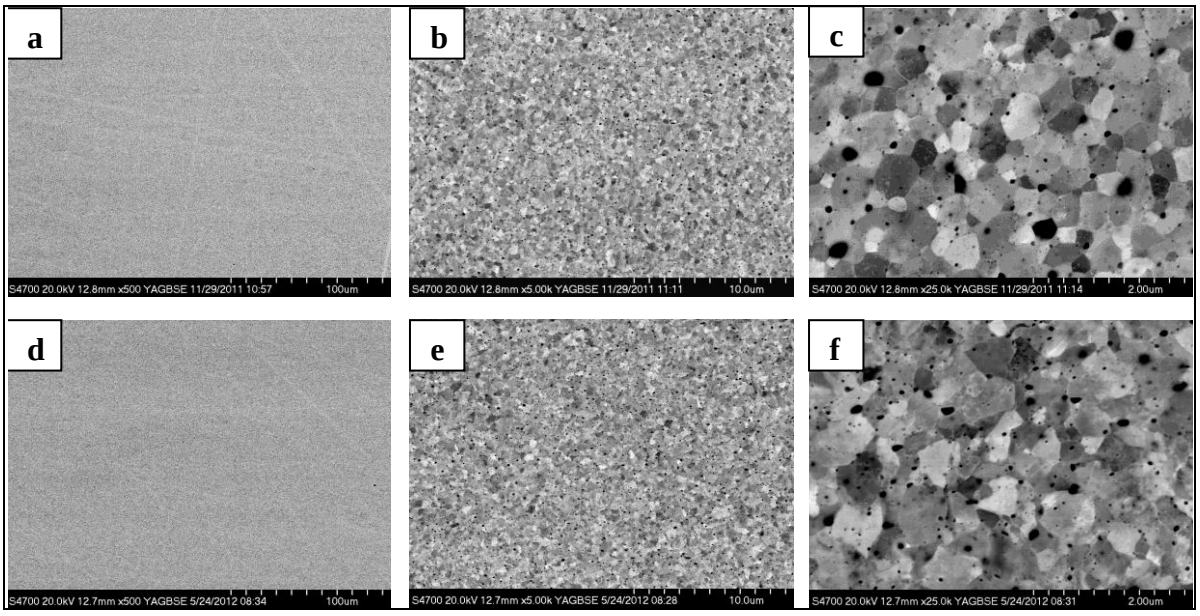

Figure 12. Micrographs of nano-tungsten sample NT3 taken at 500×, 5000×, and 25,000× magnification as processed (a, b, and c) and after Gleeble testing at 1100 °C (d, e, and f).

There did not appear to be any change in the grain size of the nano-tungsten samples without rhenium after Gleeble testing. However, due to fewer large pores in figure 12 (image f compared to image c), sample porosity may have decreased after testing. While it is not clear how representative these images are of the whole sample, this sample did exhibit a small increase in density after testing (all of the nano-tungsten did show increases in density after testing, albeit insignificantly small changes). It is possible that some porosity was closed during testing. At high magnification there does seem to be signs of grain flow (see the circled area in figure 13) at 1100 °C with some of the grains showing signs of being elongated and realigned. These grains were observed in the direction of compression (the longitudinal plain parallel to the loading direction), along the edge of the sample, and only at high magnification (25,000×).

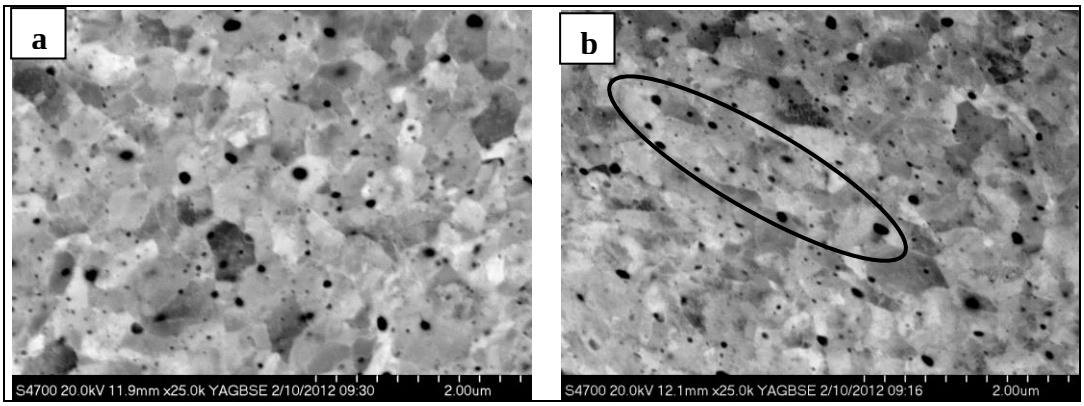

Figure 13. Images taken at 25,000× magnification of nano-tungsten sample NT3 tested at 1100 °C from the center of the sample (a) and the edge of the sample (b).

4.6.2 Tungsten With Rhenium

Figure 14 shows the microstructures of the tungsten 5% rhenium sample S3 as processed and after Gleeble testing at 1300 °C, while figure 15 shows the microstructures for the tungsten 10% rhenium sample T3 as processed and after Gleeble testing at 1200 °C.

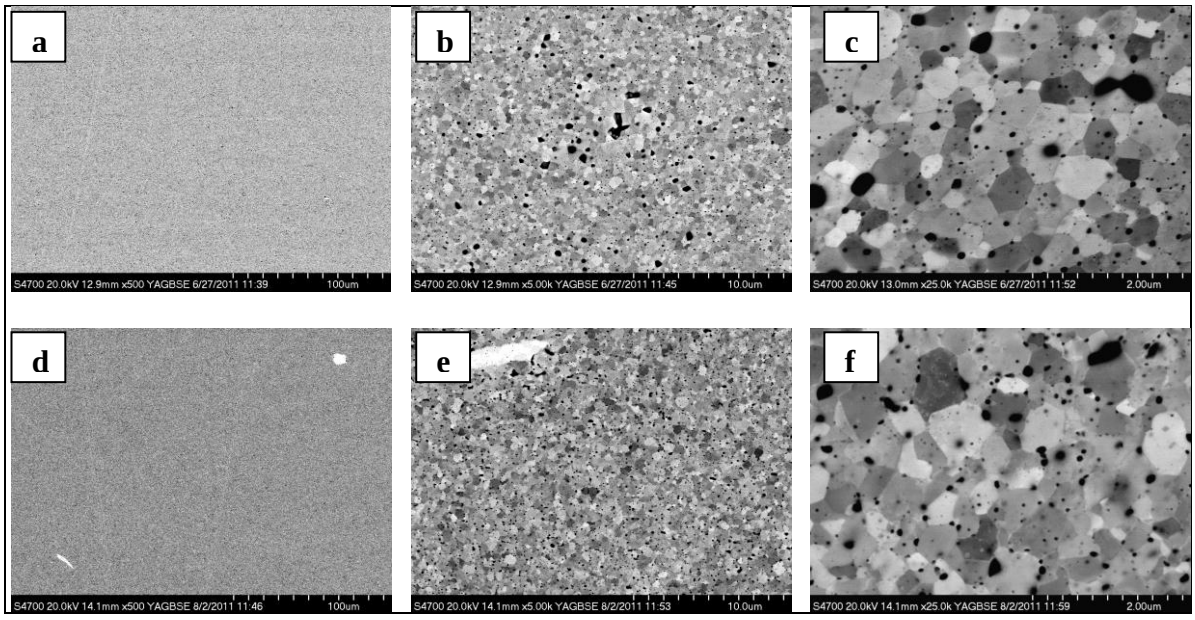

Figure 14. Micrographs of nano-tungsten 5% rhenium sample S3 as processed (a, b, and c) and after Gleeble testing at 1300 °C (d, e, and f) taken at 500×, 5000×, and 25,000× magnification.

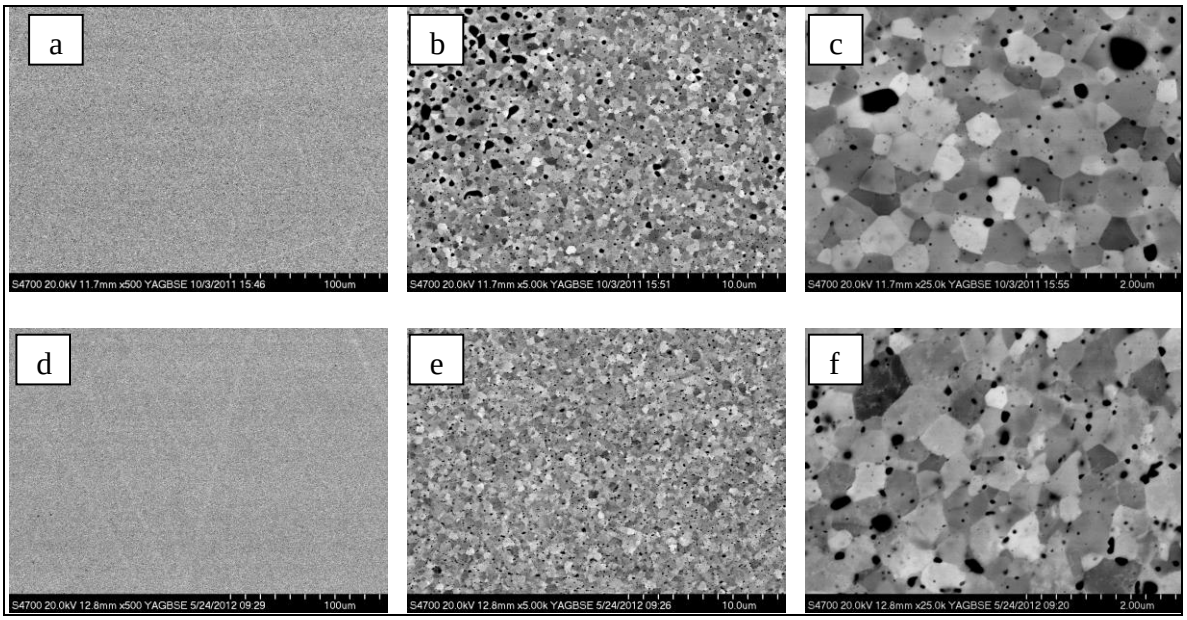

Figure 15. Micrographs of nano-tungsten sampleT3 with 10% rhenium as processed (a, b, and c) and after testing (d, e, and f) at 1200 °C taken at 500×, 5000×, and 25,000× magnification.

The nano-tungsten samples with rhenium, both 5% and 10%, did not show any microstructural changes, either in size or flow. There may have been some changes in porosity as the high magnification images in figures 14 and 15 do appear to show fewer large pores. However, both of these samples showed decreases in density after testing, making it unclear whether or not any porosity was closed off during testing. Also, it is not clear how representative these micrographs are of each sample. If there are changes in the porosity of the 5% and 10% rhenium samples, it is not as evident as in the unalloyed nano-tungsten samples. This suggests that the rhenium adds stability to the microstructure and may inhibit strain localization and provide better mechanical properties than pure nano-tungsten. However, Butler et al. (*9*) has shown that rhenium does not inhibit strain localization, at least in the case of room temperature tests, and may actually assist in localization by providing the ductility required to achieve localization at low temperatures (*9*). Furthermore, the microstructural changes observed in the localized regions of polished specimens are very subtle and may have been overlooked in this study. There are some large rhenium agglomerates present in the 5% rhenium sample micrographs that are not present in the 10% rhenium sample micrographs. These regions of high rhenium concentration could result in the formation of hard σ phase precipitates (WRe), which have been shown to strengthen the material at the expense of room temperature ductility (*10*). This may be the reason that the 5% rhenium samples exhibited a higher yield stress at elevated temperatures than the 10% rhenium samples.

4.6.3 Commercial Tungsten

Figures 16–18 show the microstructures of the as processed commercial tungsten samples.

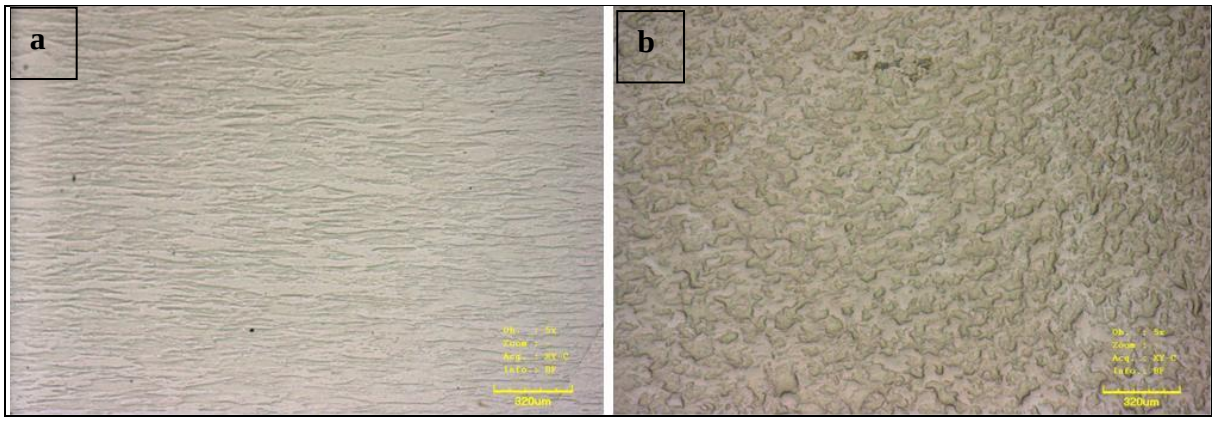

Figure 16. Optical micrographs of the commercial tungsten sample taken with a 5× objective lens in the compression direction (a) and transverse direction (b).

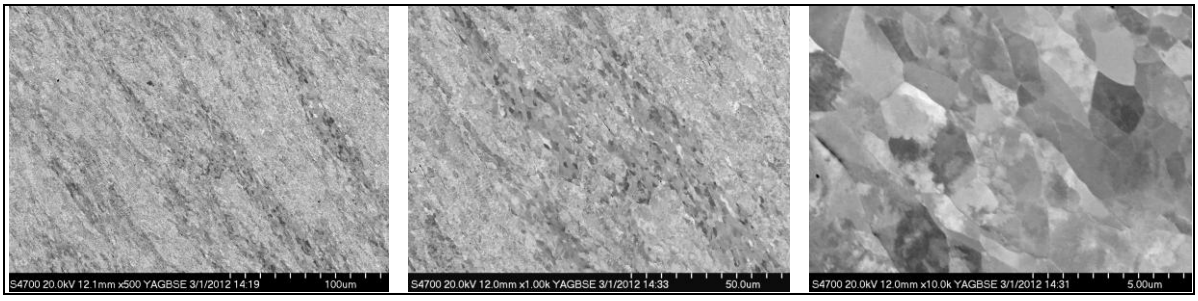

Figure 17. Micrographs of the commercial tungsten sample in the compression direction taken at 500×, 1000×, and 10,000× magnifications.

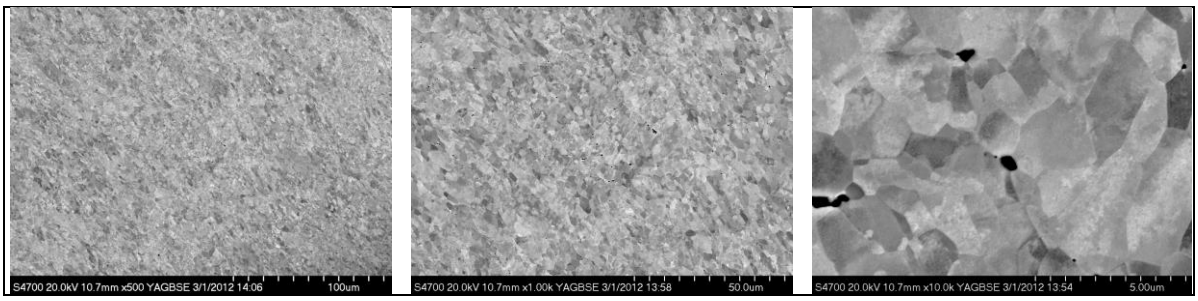

Figure 18. Micrographs of the commercial tungsten sample in the transverse direction taken at 500×, 1000×, and 10,000× magnification.

After Gleeble testing at 1200 °C, the commercial tungsten sample, B3, did not show any change in grain size in the compression direction but did show grain size reduction and grain flow (figure 19) in the transverse direction (perpendicular to the compression direction).

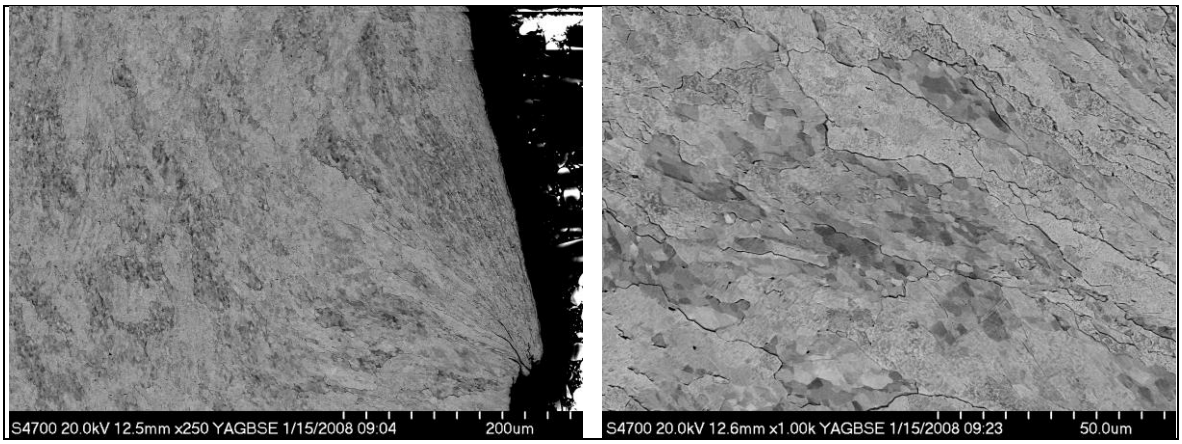

Figure 19. Micrographs of commercial tungsten sample B3 at 250× and 1000× magnifications after Gleeble testing at 1200 °C.

The grains can be seen to have changed their alignment and appear to be bending towards the barreling direction. The commercial tungsten sample showed more microstructural change than the nano-tungsten sample, which correlates well with the lower mechanical strength exhibited by the commercial tungsten.

5. Conclusions

The results of the Gleeble testing followed the expectation that the nano-grained tungsten was stronger and less ductile than the conventional commercial tungsten sample at temperature. By adding 5% and 10% rhenium to the nano-tungsten it was possible to increase the material strength and to retain more strength at higher temperatures. The addition of rhenium also improved grain stability. There was no grain growth or flow evident in the nano-tungsten samples with rhenium while grain flow, but not growth, was observed in the nano-tungsten sample. Grain refinement and flow were observed in the commercial tungsten sample.

Under the chosen test parameters the Gleeble did not provide the post-processing needed to further densify the sintered tungsten samples. While the Gleeble could easily reach the test temperatures desired and could deform the tungsten samples, there are areas for improvement. At temperatures above 1200 °C, there were problems with the anvils softening during testing. This could be overcome with improved diffusion barriers and anvils with better high temperature strength and/or reduced resistive heating. These changes could improve the simulation of post-processing conditions at the high temperatures required for conventional deformation processing of tungsten (the first steps in the forming process generally occur between 1500 and 1700 °C with each subsequent step occurring at lower temperatures [*3*]). These improvements would allow for the effective processing of nano-tungsten and nano-tungsten alloys to achieve superior strength, ductility, and fracture toughness for room temperature applications.

With proper processing controls, rhenium can dramatically improve the ductility of nano-tungsten. At room temperature, the 10% rhenium sample showed almost as much ductility as the commercial tungsten sample; neither sample cracked until reaching strain values of ~0.25, much higher than for the 5% rhenium or the unalloyed nano-tungsten sample. Unfortunately, it is difficult to remove the effects of microstructural defects and residual porosity when determining the high-temperature properties and processability of these nano-tungsten samples. Lower-temperature testing (below 1000 °C) needs to be investigated to accurately identify the ductile-to-brittle transition temperatures of nano-tungsten and nano-tungsten alloys.

6. References

1. Fang, Z.; Wang, H. Densification and Grain Growth During Sintering of Nanosized Particles. *International Materials Reviews* **2008**, *53* (6), 326–352.

2. Butler, B.; Klier, E.; Kelly, M.; Gallagher, M. *Thermal Stability of Milled Nanocrystalline Tungsten Powders*; ARL-TR-5541; U.S. Army Research Laboratory: Aberdeen Proving Ground, MD, 2011.

3. Lassner, E.; Schubert, W. D. *Tungsten: Properties, Chemistry, Technology of the Element, Alloys, and Chemical Compounds*; Kluwer Academic and Plenum Publishers: New York, 1999; p 256.

4. Ma, E. Eight Routes to Improve the Tensile Ductility of Bulk Nanostructured Metals and Alloys. *JOM Journal of the Minerals, Metals and Materials Society* **2006**, *58* (4), 49–53.

5. Klopp, W. D.; Holden, F. C.; Jaffee, R. I. *Further Studies on Rhenium Alloying Effects in Molybdenum, Tungsten, and Chromium;* Battelle Memorial Institute: Columbus, OH, 1960.

6. Myhr, O.; Grong, O.; Fjaer, H.; Marioara, C. Modeling of the Microstructure and Strength Evolution in Al-Mg-Si Alloys During Multistage Thermal Processing. *Acta Materialia* **2004**, *52* (17), 4997–5008.

7. Mintz, B.; Arrowsmith, J. Hot Ductility Behaviour of C-Mn-Nb-Al Steels and Its Relationship to Crack Propagation During the Straightening of Continuously Cast Strand. *Met. Technology* **1979**, *6* (1), 24–32.

8. Stephens, J.; Form, G. *Strain Aging Effects in Tungsten Due to Carbon;* NASA TM X-5200; Lewis Research Center: Cleveland, OH, 1964.

9. Butler, B.; Klier, E.; Casem, D.; Dwivedi, A.; Gallagher, M.; Hays, J. *Demonstration of Shear Localization in Ultrafine Grained Tungsten Alloys via a Powder Metallurgy Processing Route*; ARL-TR-6214; U.S. Army Research Laboratory: Aberdeen Proving Ground, MD, 2012.

10. Jaffee, R. I.; Sims, C. T. *The Effect of Rhenium on the Fabricability and Ductility of Molybdenum and Tungsten;* Battelle Memorial Institute: Columbus, OH, 1958.

NO. OF
COPIES ORGANIZATION

1 (PDF only) DEFENSE TECHNICAL INFORMATION CTR
DTIC OCA
8725 JOHN J KINGMAN RD
STE 0944
FORT BELVOIR VA 22060-6218

1 DIRECTOR
US ARMY RESEARCH LAB
IMAL HRA
2800 POWDER MILL RD
ADELPHI MD 20783-1197

1 DIRECTOR
US ARMY RESEARCH LAB
RDRL CIO LL
2800 POWDER MILL RD
ADELPHI MD 20783-1197

ABERDEEN PROVING GROUND

9 DIR USARL
RDRL WMM
R DOWDING
RDRL WMM D
K CHO
RDRL WMM F
F KELLOGG (2 CPS)
B BUTLER
S GRENDAHL
E KLIER
L KECSKES
H MAUPIN

INTENTIONALLY LEFT BLANK.